



DATA PAPER

Open Access



Traceability and quality assessment of Norway spruce (*Picea abies* (L.) H.Karst.) logs: the TreeTrace_spruce database

Fleur Longuetaud^{1*} , Rudolf Schraml^{2,3}, Frédéric Mothe¹, Tojo Ravoajanahary¹, Rémi Decelle^{1,4}, Thiéry Constant¹, Phuc Ngo⁴, Isabelle Debled-Rennesson⁴, Karl Entacher^{3,5}, Alexander Petutschnigg⁵, Franka Brüchert⁶ and Andreas Uhl²

Abstract

Key message The *TreeTrace_spruce* database contains images and measurements of 100 Norway spruce (*Picea abies* (L.) H.Karst.) logs from Northeastern France, each about 4.5 m long. The image database includes RGB images of large and small ends of the logs and hyperspectral and computed tomography (CT) images of wood discs sampled at both log ends. The 100 logs were also fully X-ray scanned with a CT device for roundwoods and their top surface was scanned with a terrestrial LiDAR device. The measurements performed on discs include wood local density, growth ring widths and pith location. This database is complementary to another one (*TreeTrace_Douglas*) resulting from the same ANR project *TreeTrace*, but if the objectives are similar, the protocols and conditions of acquisition are not the same for these two databases. *TreeTrace_spruce* dataset is available at <https://doi.org/10.57745/WKLTJI> and associated metadata are available at <https://metadata-afs.nancy.inra.fr/geonetwork/srv/fre/catalog.search#/metadata/cffe2f1-18e1-4b53-9f5b-6cc4c66f1cb8>.

Keywords Image analysis, RGB images, Computed tomography, *Picea abies*, Wood density, Growth ring width, Terrestrial LiDAR

1 Background

In this article, we present the database called *TreeTrace_spruce*. This database mainly contains RGB, hyperspectral and CT images of Norway spruce (*Picea abies* (L.) H.Karst.) log ends. Images of untreated log ends (i.e. freshly sawn without any further preparation like sanding and polishing) were collected in this project. Wood quality features such as pith position, growth ring widths and local wood density were measured on discs sampled at both log ends. CT and LiDAR scanning were performed directly on the logs.

The data were collected in the framework of the *TreeTrace* project (ANR-17-CE10-0016). The choice of species in the *TreeTrace* project is related to the fact that the species Norway spruce and Douglas fir are of major importance in the three countries participating

Handling Editor: Véronique Lesage.

*Correspondence:

Fleur Longuetaud
fleur.longuetaud@inrae.fr

¹ Université de Lorraine, AgroParisTech, INRAE, Silva, 54000 Nancy, France

² Department of Computer Sciences, University of Salzburg, 5020 Salzburg, Austria

³ Holztechnikum Kuchl, 5431 Kuchl, Austria

⁴ Université de Lorraine, CNRS, LORIA, F-54000 Nancy, France

⁵ Department of Forest Products Technology and Timber Construction, University of Applied Sciences Salzburg, 5412 Puch-Urstein, Austria

⁶ Department of Forest Utilisation, FVA Baden-Württemberg, 79100 Freiburg, Germany



© The Author(s) 2023. **Open Access** This article is licensed under a Creative Commons Attribution 4.0 International License, which permits use, sharing, adaptation, distribution and reproduction in any medium or format, as long as you give appropriate credit to the original author(s) and the source, provide a link to the Creative Commons licence, and indicate if changes were made. The images or other third party material in this article are included in the article's Creative Commons licence, unless indicated otherwise in a credit line to the material. If material is not included in the article's Creative Commons licence and your intended use is not permitted by statutory regulation or exceeds the permitted use, you will need to obtain permission directly from the copyright holder. To view a copy of this licence, visit <http://creativecommons.org/licenses/by/4.0/>.

in the project. In France, they represent the largest standing volumes and the highest annual growth, as well as the largest volumes produced by sawmills (FCBA 2022). In Austria and Germany, too, spruce is the most important wood species (BFW 2022) and Douglas fir is one of the promising climate change species in both countries (BFW 2008).

This article and the corresponding database are complementary to the article already published on the Douglas fir part of the project (Longuetaud et al. 2022a) and the associated database *TreeTrace_Douglas fir* (<https://doi.org/10.15454/YUNEGE>). The general objectives described below are similar but the protocols, data types and acquisition conditions differ between the two databases and it was important to distinguish the two samplings. The main differences between the two databases are as follows:

- *TreeTrace_Douglas*: The database was collected in an industrial context with RGB images taken on the log yard of a sawmill and then on the sawing line with an industrial camera installed for the project. Moreover, as this was a strong originality of this database, boards were collected and sent to the LaBoMaP laboratory (Arts et Métiers Sciences et Technologies, Cluny) to be analysed in terms of mechanical quality with the final objective of linking the quality information obtained on the logs and then on the boards;
- *TreeTrace_spruce*: The database was collected at the felling site and then at the FVA (Forest Research Institute Baden-Württemberg, Freiburg, Germany), with acquisition of terrestrial LiDAR images of the surface of the logs and CT images on the whole length of the 4.5 m logs that were scanned through the Microtec X-ray scanner at FVA. This point constitutes a strong originality of this database with the possibility of linking the external observations with the internal structure of the logs. In addition, hyperspectral images are also available for this species.

In the context of climate change and strong pressure on resources, the optimisation of the forest and wood sectors is a challenge. In order to make the best use of wood resources and ensure supplies to industries in terms of both quality and quantity, it is necessary to be able to describe the quality of the resource as early as possible in the processing chain and to develop the traceability of this resource. Moreover, in the context of illegal logging, there is an increasing need to trace logs.

The data collected from the spruce sample of the *TreeTrace* project can be used for several purposes:

- Wood traceability along the forest wood chain, from the forest to the sawmill, by image processing of cross-sections only, potentially based on techniques such as those used for fingerprint recognition.
- Assessment of the wood quality based on cross-section analysis mainly, applicable in the forest, on a log sorting platform or at the sawmill. The information available on a cross-section (geometric centre, pith location, juvenile wood area, number and width of the annual growth rings) is complementary to what could be obtained from the analysis of the external log shape by laser sensors installed at the entrance of the sawing line (in practice, only tapering information is generally used).

These application cases share many aspects. A common dataset for experimental validation can be used, ground-truth data established by annotating images can be shared and many software components implementing preprocessing (e.g. pith detection, cross-section segmentation, contrast optimization) as well as feature extraction techniques (e.g. annual ring detection) can be developed jointly and shared subsequently.

In the literature, very few references propose algorithms for image processing of untreated log ends. Some algorithms exist for images of sanded and polished cross-sections in the context of dendrochronology but these algorithms are not made to process images of rough log end sections. First application on untreated log end images is to segment the wood cross-section in the entire image. The method proposed by Schraml and Uhl (2014) to segment wood cross-sections of spruce is a similarity-based region growing algorithm and requires pith location. Their main objective was to trace log ends from the forest to the sawmill (Schraml et al. 2015). More recently, neural networks were used to perform this task (Wimmer et al. 2021a). A second application is to estimate the pith location. Norell and Borgfors (2008) have estimated the pith location in order to further detect tree rings (Norell 2011). Schraml and Uhl (2013) and Kurdthongmee et al. (2018) proposed algorithms for pith detection on digital images of untreated wood cross-sections. For Schraml and Uhl (2013), the objective was to retrieve cross-section characteristics in order to trace log ends. Recently, Deep Neural Networks (DNNs) were trained in order to address the problem of the pith detection in cross-section images of logs (Kurdthongmee 2020).

The work already carried out with the *TreeTrace_spruce* database is listed in Section 5.

2 Methods

2.1 Log sampling in the field

The sampling was performed in a Norway spruce even-aged stand located near Corcieux, France (48.1968 N; 6.8869 E). The trees were approximately 55 years old. No information was available about the silvicultural history of the stand. A clear cut was performed a few days before our sampling on September 24 and 25, 2018. Since the logs were left in piles, it was not possible to know which logs belonged to the same tree (Fig. 1). The logs came from different heights in the trees. We selected 100 logs of 4.5-m length, rejecting logs with very large visible defects. The logs have been labelled *E001* to *E100*. The number of rings counted at the log ends (see Section 2.8) allowed to estimate the height in the stem of the logs (Ravoajanahary et al. 2022). We concluded that the logs came from three heights in the tree: approximately 0m, 4.5m and 9m. Consequently the corresponding discs sampled at both log ends (Section 2.8) came from four heights in the tree: approximately 0m, 4.5m, 9m and 13.5m (Fig. 2).

2.2 Image acquisition in the field in Corcieux (set #1)

RGB images of large and small log ends were taken using two devices: a Panasonic FZ45 Lumix camera ($f/3.2$ aperture, focal length 4.5 mm) and a Huawei P8 Lite 2017 smartphone ($f/2.2$ aperture, focal length 3.8 mm). At least five images of each log end were taken with each device: Two images taken with the same orientation, two images taken after tilting the camera by around 45° , then a last image after stapling the label on the cross-section (Fig. 3). In total, 1009 images (4320×3240 pixels) taken with the Lumix camera and 1013 images (3968×2976 pixels) taken with the Huawei smartphone were obtained at Corcieux (Table 1). The images (raw and with labels) are available on the data repository in `TreeTrace_spruce/log_end_images/RGB/Corcieux_Lumix` and `TreeTrace_spruce/`

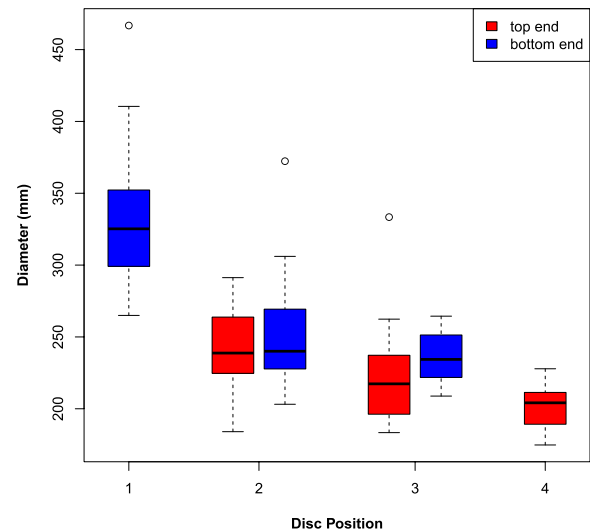


Fig. 2 Diameter of the discs as a function of their height level in the tree and their location in the sample logs (large end or small end). Height levels 1, 2, 3 and 4 correspond to heights 0m, 4.5m, 9m and 13.5m, respectively

`log_end_images/RGB/Corcieux_Huawei`. A 25-cm-long calibration scale of $1\text{ cm} \times 1\text{ cm}$ black and white squares was included in each photo (Fig. 3).

For a subset of 100 images (one image of the large end of each of the 100 logs taken with the Lumix device), the pixel widths in millimeters are given by the variable `pixelWidth_mm`. For each of these 100 images, a manual processing was done to locate the pith (`pithX_pixel` and `pithY_pixel`) and to delineate the outline of the wood cross-section under-bark. The segmented images are available in `TreeTrace_spruce/log_end_images/RGB/Corcieux_Lumix/segmented/large_ends`. For each image, the under-bark area of the wood cross-section in pixels was computed (`areaUB_pixel`). All the *RGB image-level* data are in the file `TreeTrace_spruce/tables/rgb_images.txt`.



Fig. 1 Logs immediately after harvesting (on the left). The 100 selected logs ready for photographing and labelling (on the right)

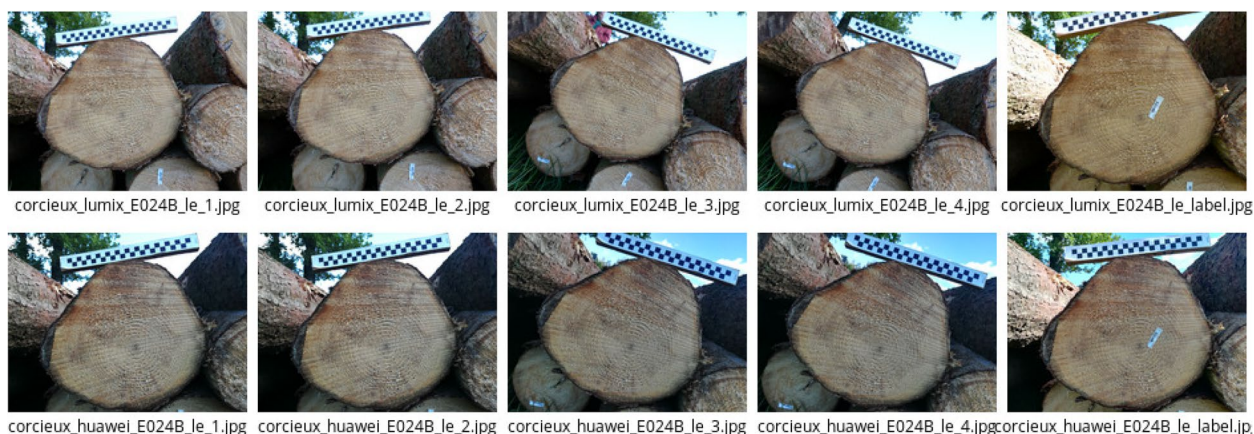


Fig. 3 RGB images of cross-section *E024B_le* taken with Lumix device (first row) and Huawei device (second row) at Corcieux

Table 1 Number of RGB images taken at each site and with each camera at both ends of the 100 sampled logs

Site	Set	Camera		Large end	Small end
Corcieux	1	Lumix camera	Raw	403	406
			Labels	100	100
		Huawei smartphone	Raw	411	402
			Labels	100	100
Freiburg	2	Huawei smartphone	Raw	270	290
			Labels	100	100
Munich and Kuchl	3	Canon camera	Raw	399	376
			Sanded	644	658

2.3 Naming conventions

Labels were stapled at both ends with the log number followed by a letter *B* or *H* to indicate the bottom (*B*) or top (*H*) side of the log. But since the log taper was not always very pronounced, several errors occurred: Logs *E019*, *E027*, *E032*, *E057*, *E062*, *E071*, *E072*, *E075*, *E087*, *E089*, *E090*, *E094* were thus mislabelled with *H* on bottom side and *B* on top side. These wrong names are the ones that appear on the RGB images taken after stapling the labels (fifth column in Fig. 3).

To avoid confusion, all the logs have been renamed in this database with suffixes *_le* and *_se* to indicate the actual large end (bottom side) and small end (top side) of the log, respectively. For instance, large end of log *E024* was renamed *E024B_le* and large end of log *E019* (mislabelled with *H*) was renamed *E019H_le*.

The image files were named with respect to site, camera device, log name, log end and image number. For instance, *corcieux_lumix_E024B_le_3.jpg* refers to the third image of large end of log *E024* taken with the Lumix device at Corcieux site, and *corcieux_lumix_E024B_le_label.jpg* is the image of the same cross-section after stapling the label.

2.4 Wood disc sampling and image acquisition in Freiburg (set #2)

The logs were then delivered to the Forest Research Institute of Baden-Württemberg (FVA) at Freiburg, Germany, on September 26, 2018, by a transporter. On September 27 and 28, discs of about 5 cm thick were cut at both ends of each log (200 discs in total). The discs were then kept fresh in plastic film. The measurements that have been made on discs are presented in Section 2.8.

After refreshing the log ends by cutting the discs, a new set of RGB images of both log cross-sections was taken with the Huawei smartphone. Several images were taken of each log end: One image with the label before cutting the disc, then one to three images of the fresh section after cutting the disc by changing the orientation of the camera (Fig. 4). In total, 760 images (3968 × 2976 pixels) taken with the Huawei smartphone were obtained at Freiburg (Table 1) and are available on the data repository in *TreeTrace_spruce/log_end_images/RGB/Freiburg_Huawei*. A 25-cm-long calibration scale of 1 cm × 1 cm black and white squares was included in each photo.

As it was done for the images taken at Corcieux (Section 2.2), for a subset of 100 images (one image of the



freiburg_huawei_E024B_le_label.jpg freiburg_huawei_E024B_le_1.jpg freiburg_huawei_E024B_le_2.jpg freiburg_huawei_E024B_le_3.jpg
Fig. 4 RGB images of cross-section *E024B_le* taken with Huawei device at FVA Baden-Württemberg (Freiburg). The first image (left) was taken before cutting the disc, the other three after cutting the disc

large end of each of the 100 logs), the pixel widths in millimeters are given by the variable *pixelWidth_mm*. For each of these 100 images, a manual processing was done to locate the pith (*pithX_pixel* and *pithY_pixel*) and to delineate the outline of the wood cross-section under-bark. The segmented images are available in `TreeTrace_spruce/log_end_images/RGB/Freiburg_Huawei/segmented/large_ends`. For each image, the under-bark area of the wood cross-section in pixels was computed (*areaUB_pixel*). All the corresponding RGB image-level data are in the file `TreeTrace_spruce/tables/rgb_images.txt`.

The image files were named with respect to site, camera device, log name, log end and image number. For instance, *freiburg_huawei_E024B_le_3.jpg* refers to the third image of large end of log *E024* taken with the Huawei device in Freiburg.

2.5 Terrestrial LiDAR scanning of logs

After cutting the discs, the logs were scanned using a T-LiDAR device (Faro Focus 3D X130). The logs were placed on the ground over two supports by sets of 20 logs

that were scanned together. Four scans were performed for each set (Fig. 5). Each scan took 15 min with a resolution of 20,000 points/turn such as the distance between two cloud points was 3 mm at 10 m of distance. The scene was restricted to the area around the logs. No noise filtering was applied to the cloud points.

Several large diameter spheres were used for helping to merge the obtained clouds of points and small diameter spheres were placed on each log for helping the matching between T-LiDAR scans and CT scans (Figs. 5 and 6).

Figure 7 shows the preview of a T-LiDAR cloud of points. It should be noted that the bark of the logs was relatively damaged by the harvester and transportation. Point clouds registration was performed using Faro Scene 5.4 software taking position 4 as reference. In the end, five merged point clouds, one for each set of 20 logs, are available on the data repository in `TreeTrace_spruce/log_images/tlidar`. The cloud files are in text format with XYZ coordinates (in meters, Z corresponding to the altitude) and a reflectance value (given as an RGB triplet). The `log_order_and_position.txt` file gives the position of the logs in each cloud and

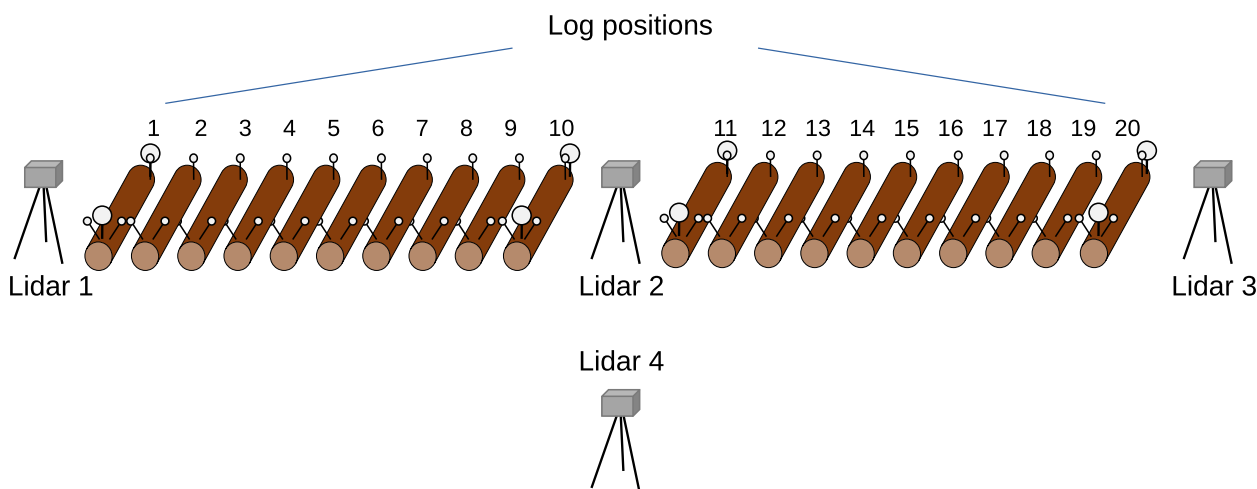


Fig. 5 Locations of the device for T-LiDAR scanning



Fig. 6 A set of logs ready for T-LiDAR scanning and T-LiDAR device in place at location 3



Fig. 7 T-LiDAR view of a set of 20 logs scanned from location 3

the disc identifiers corresponding to the log ends oriented toward position 4 in Fig. 5.

2.6 X-ray scanning of logs

CT scanning was performed immediately after T-LiDAR scanning at FVA Baden-Württemberg (Fig. 8) with the CT.Log (MiCROTEC s.r.l.) scanner as described in Stänkle et al. (2015).

The logs were scanned at a generator voltage of 180 kV and a generator current of 14 mA. The scanning direction follows the log from the larger (butt) end to the smaller (top) end. The CT images were reconstructed to an axial resolution of 4.8 mm or 5 mm and a resolution of 1.107 mm × 1.107 mm in the planes perpendicular to the axial direction. The nominal length of each log extractable from the CT scan is shorter than the physical log length as 11 slices on the butt end and 13 slices from the top end were cut due to the layout of the scanner with metal holders of high material density which interferes with the log density as such. The image files of the reconstruction `TreeTrace_spruce/log_images/xray/tif` are named in consecutive order according to the original log

ID. The reconstruction files are 8-bit greyscale multipage tiff-files, with each page representing one log slice. The resolution of each page is 768 by 768 pixels. A second image dataset `TreeTrace_spruce/log_images/xray/segmented` contains a semantic segmentation of the features of each log, which were detected in the CT scans. The images are 8-bit greyscale multipage tiff-files, too, with individual grey levels for each of the following five features: Air (area outside log): 255; bark: 150; sapwood: 200; heartwood: 250; pith: 10; region of sound knot:100; region of dead knot: 50. The feature detection was based on the CT.Pro software package (Version Dez-2015).

2.7 Hyperspectral and RGB imaging of the discs before and after sanding in Munich (set #3)

The discs were then transported to Stemmer Imaging (<https://www.stemmer-imaging.com/>) in Munich, Germany. During transport and intermediate storage, the discs were packed individually in plastic bags to avoid surface cracks due to wood shrinkage and discoloration due to oxidation processes (see Fig. 9b).



Fig. 8 Installation of a log for CT scanning

At Stemmer Imaging, the fresh cut side of each disc was scanned with two different multispectral line scanners and RGB images were taken. Note, that all images captured from the wood discs are mirrored versions of the images captured from the log ends.

The hyperspectral scanning setup is shown in Fig. 9a—halogen light was used for lighting. The first scanner was a so-called Specim FX10, which scans the spectra between a wavelength from 445 to 983nm with a bandwidth of approx. 3nm. The second scanner was a Specim FX17 which provides scans between 990 and 1665nm also with a bandwidth of approx. 3nm. Therefore, the Specim FX10 uses mainly the visible light (VIS) spectra and the Specim FX17 uses mainly parts of the NIR spectra. For the scanning setup, a

resolution of 640×640 pixel was chosen. Each wood disc was scanned with both cameras. For this purpose, each disc was pushed through the system by hand and the speed was synchronized with a trigger. The hyperspectral data, i.e. the translation from line scanning data to a hyperspectral cube, was performed by the acquisition software Perception Studio.

After multispectral scanning with the first camera, the same side was captured using a Canon 70D, 35mm lens. At least four images with different rotations were taken of each disc.

After hyperspectral scanning and RGB imaging the rough discs were transported to Kuchl, Austria, where each disc was sanded with a mesh width of 120 to reduce the influence of manual chainsaw cuts at scanning. This



(a) Scanning system (b) Wood disc storage (c) Hyperspectral cube cropping

Fig. 9 The sensor system shows the line scanner Specim FX10 which was mounted on a metal frame and the slice is moved perpendicular to the scanned line manually. The stored samples were closed airtight to avoid surface changes. Each hyperspectral cube was cropped to reduce the massive amount of data

mesh width was chosen as it gave good results for the wet samples. In Kuchl RGB images were taken using the same setup as in Munich—at least six images with different rotations were taken.

In total, 2077 images (4320×3240 pixels) taken with the Canon camera at Munich and Kuchl were collected (Table 1). The images are available on the data repository in `TreeTrace_spruce/log_end_images/RGB/Munich_Canon`.

The hyperspectral data (captured with the FX10 or FX17 camera) from each disc were stored in a special format (HSD – hyperspectral data) utilized by Perception Studio. A HSD file contains all spectral bands of a disc in kind of a hyperspectral cube. It was necessary to convert the data to the ENVI format for which open source image processing libraries are available.

The ENVI files for the 200 discs are provided in the repository under the following path: `TreeTrace_spruce/log_end_images/hyperspectral`.

2.7.1 Notes on the hyperspectral data

Figure 10 provides exemplary images for one wood disc (#E001B). In the first and second row RGB images taken from the raw and sanded disc surface are shown. In the subsequent rows, for each hyperspectral camera, images for selected bands are illustrated for the same disc, raw and sanded.

It can be recognized that the width of the wood disc for the FX10 and FX17 images differs. We assume that this is caused by the acquisition software and an inaccurate trigger synchronization. Furthermore, a set of cubes got lost during file storage and are thus missing in the repository. Table 2 shows an overview of the number of captured cubes for each hyperspectral camera. For the FX10 and the raw discs all cubes are available.

2.8 Measurements on wood discs

Finally, the 200 discs were transported to INRAE Nancy, France, in March 2019, for further analyses. Ring widths were measured on four orthogonal radii and are provided in the *disc-radius-ring-level* data file (`TreeTrace_spruce/tables/discs_radii_rings.txt`). From these values, the average profile of annual ring widths of a disc was obtained by subtracting the successive quadratic means of the four radii (i.e. root mean square of external radii of a given ring minus root mean square of internal radii of the same ring). The corresponding *disc-ring-level* data file (`TreeTrace_spruce/tables/discs_rings.txt`) provides cambial age (*cambialAge*), growth year (*growthYear*), distance to pith (*externalRadius_mm*) and ring width (*ringWidth_mm*).

Then, the discs were scanned in air-dried state with the medical CT scanner described in Freyburger et al. (2009). *202 CT images are available* since two discs were scanned in two pieces. CT images, raw (DICOM) and calibrated in density (following the method described in Freyburger et al. (2009)), are provided on the data repository in `TreeTrace_spruce/log_end_images/xray`.

CT images were then processed as described in the *Image processing* section of Longuetaud et al. (2016) with the exception that only air-dried state was considered. This method makes it possible to output air-dried-specific gravity in tangential bands of fixed mean width and divided in several azimuthal sectors for the analysis of radial variations for example. Here, the mean width of the tangential bands was set to 1mm and the bands were not divided azimuthally. A radial profile of air-dried density consisting of the average distance to the pith (*meanRadius_mm*) and density (*airDryDensity_kgpm3*) of each tangential band is thus obtained for each disc (`TreeTrace_spruce/tables/discs_density_profiles.txt`).

The radial profile of ring widths was coupled with the radial profile of density to assess the mean density of each annual growth ring (*airDryDensity_kgpm3*). The variable was added to the *disc-ring-level* data file. The method is described in Ravoajanahary et al. (2022).

These *disc-ring-level* data were used to compute the data table at the disc level (`TreeTrace_spruce/tables/discs_measurements.txt`). In this table, the average density of a disc (*airDryDensity_kgpm3*) is the average of all pixels corresponding to wood (excluding bark) in the calibrated CT image. The number of these pixels was used to compute the under-bark area of the discs (*areaLIBScanner_cm2*). The quadratic mean of the four radii on which ring widths were measured (*meanRadiusLIBOptical_mm*) is also reported. The height in the stem of each disc (*estimatedHeight_m*) was estimated based on the number of rings as explained in Section 2.1.

3 Access to the data and metadata description

The images and the database (Longuetaud et al. 2022b) are available at Recherche Data Gouv repository: <https://doi.org/10.57745/WKLTJI>. Associated metadata access is at <https://metadata-afs.nancy.inra.fr/geonetwork/srv/fre/catalog.search#/metadata/cfee2f1-18e1-4b53-9f5b-6cc4c66f1cb8>.

The arborescence of the *TreeTrace_spruce* directory was detailed in the previous section and is summarized in Fig. 11.

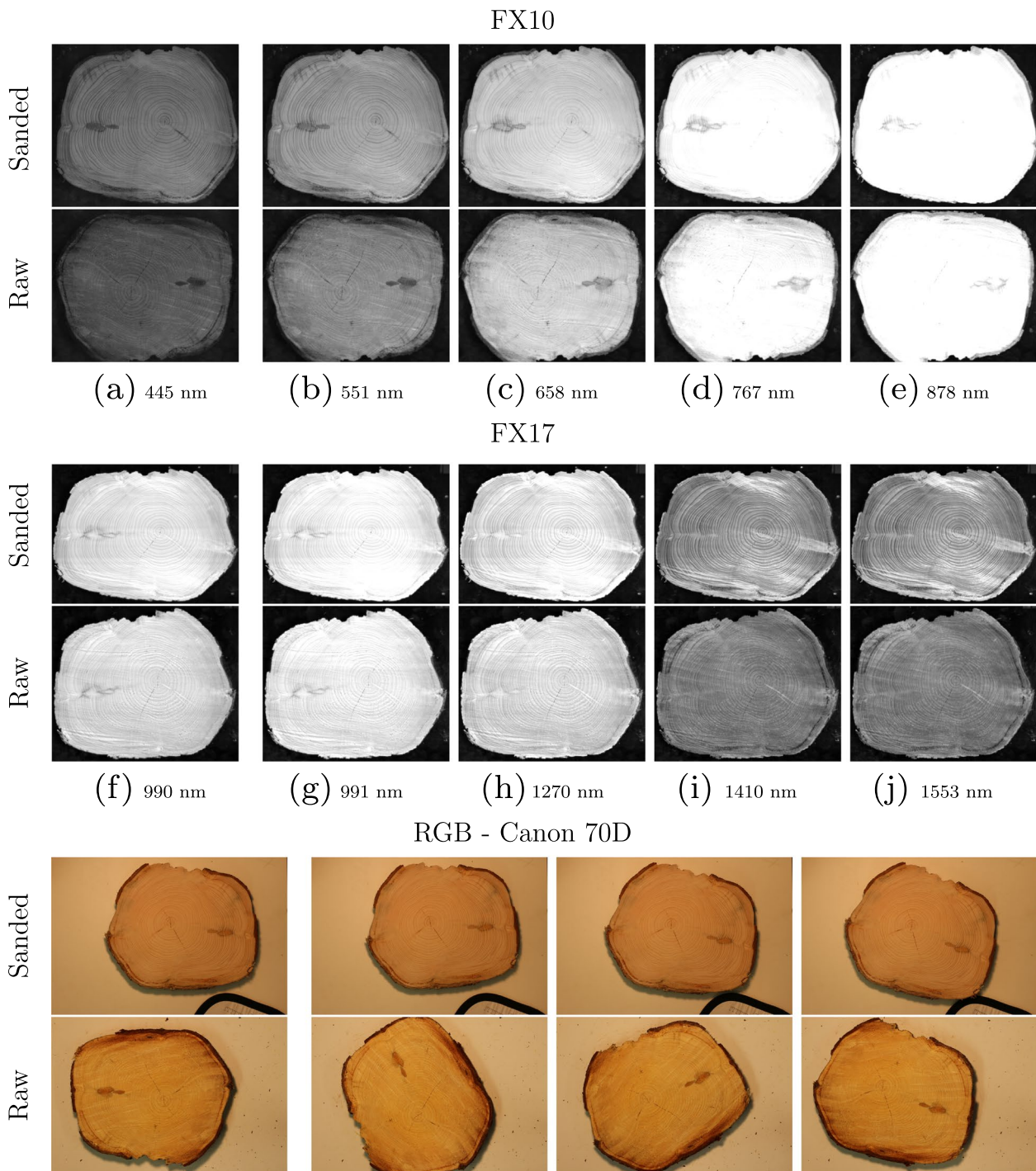


Fig. 10 Hyperspectral images of cross-section *E001B_le* taken with FX10 camera (first row) and FX17 camera (second row) and RGB images taken with Canon device (third row) at Munich

The main numeric data are in the `TreeTrace_spruce/tables` directory. There are five tables, all in the form of an array with variables in columns and a first line indicating the variable names. Each data table

is accompanied with a variable table (with the same name followed by `_variable`) describing each variable. The data tables are the following with the different levels of measurements:

Table 2 Number of hyperspectral cubes taken with each camera in rough and sanded states at both ends of the 100 sampled logs

Hyperspectral camera	Surface	Large end	Small end
FX10	Raw	100	100
FX10	Sanded	88	12
FX17	Raw	99	96
FX17	Sanded	78	9

- The `discs_measurements` table contains 200 lines, one for each disc or log end, and 7 columns.
- The `rgb_images` table contains 1164 lines, one for each image on which any measurement has been made, and 8 columns.
- The `discs_rings` table contains 8494 lines, one for each annual growth ring of each disc, and 7 columns. The variables were computed from ring widths measured on orthogonal radii and density profiles issued from CT images.
- The `discs_radii_rings` table contains 8494×4 radii = 33976 lines, one for each ring measurement on each radius, and 6 columns.
- The `discs_density_profiles` table contains 25,230 lines, one for each 1-mm-wide tangential

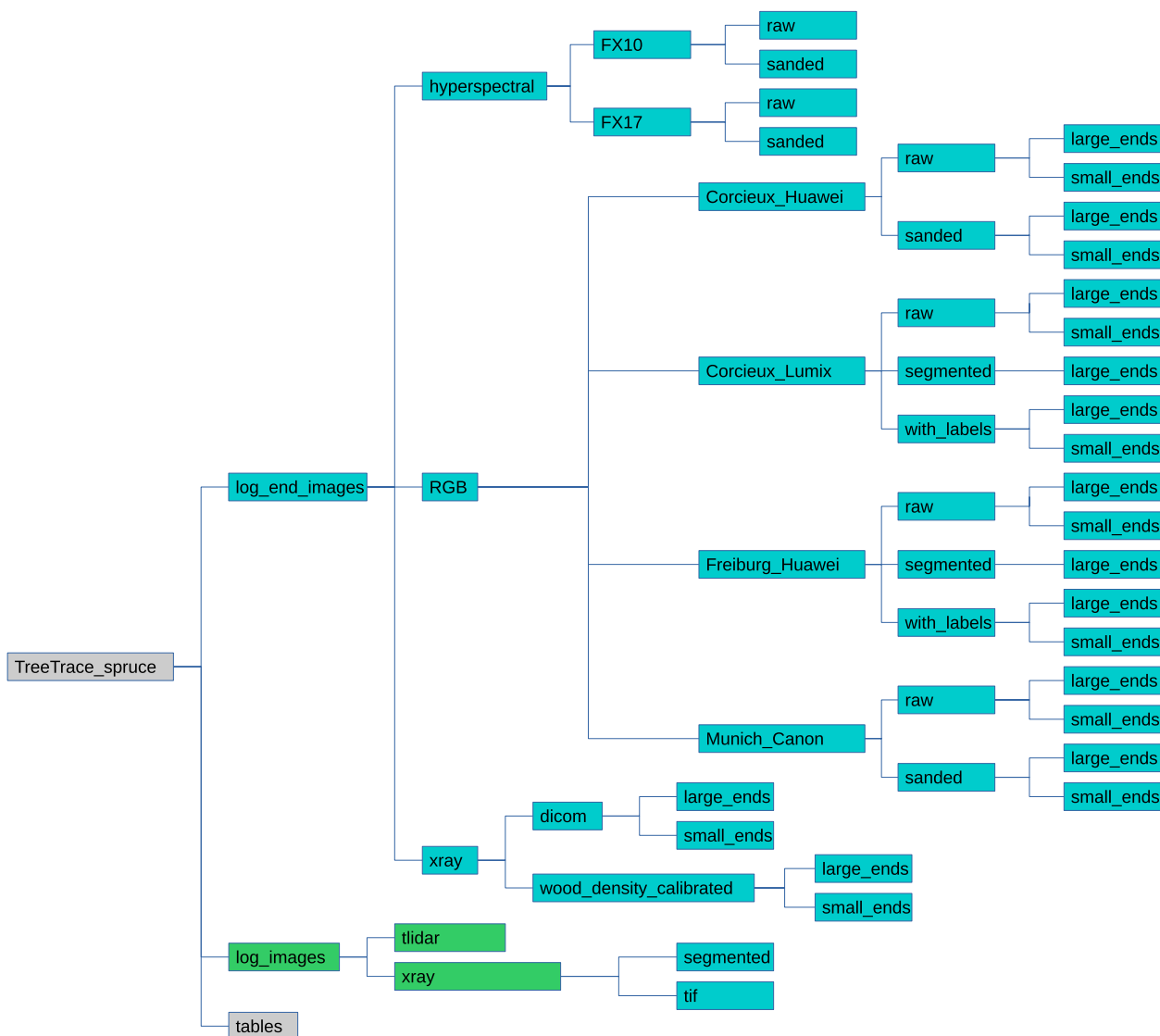


Fig. 11 Organisation of the data files

band on which air-dry density was measured on the CT images, and 5 columns.

4 Technical validation

All measurements were carefully checked by graphical analyses with R software. The ring measurements were controlled by using a binocular magnifying glass when in doubt and by checking for consistency between ring profiles from the four radii measured on each disc. The X-ray CT scanner used to measure wood density is controlled and calibrated by the manufacturer three times a year. A specific calibration procedure (Freyburger et al. 2009) was used to convert Hounsfield Units to wood density.

5 Reuse potential and limits

All data tables are in plain text format with tabulations as separator. They can be imported easily with R or with any spreadsheet software. Sometimes information is missing for some variables, which is translated in “NA” value in the tables.

The RGB images are in standard JPEG or PNG formats. A scale included in each image allows to perform spatial calibration. For a subset of RGB images (one image per log taken at the large end and per site and device), the black and white scale was manually measured in the images and the image resolution is provided in a Table.

The CT images of the discs (in the `TreeTrace_spruce/log_end_images/xray` directory) and logs (in the `TreeTrace_spruce/log_images/xray` directory) can be read with ImageJ software (<https://imagej.nih.gov/ij/>).

The registered T-LiDAR clouds (in the `TreeTrace_spruce/log_images/tlidar` directory) can be visualised with the 3D point cloud processing software CloudCompare (<https://www.danielgm.net/cc/>).

The hyperspectral images (in the `TreeTrace_spruce/log_end_images/hyperspectral` directory) require Matlab to be read.

The image database *TreeTrace_spruce*, providing both raw images and ground truth, can be used to develop and to validate image analysis algorithms for detecting various features (e.g. pith location, cross-sectional area, annual ring widths) on untreated (i.e. freshly cut) cross-sections of logs.

The main objectives for the further development of algorithms are (1) to trace the logs from the forest to the sawmill and/or (2) to estimate the wood quality directly in the forest, on the log yard or on the sawmill line before sawing. Both were objectives of the *TreeTrace* project.

The difficulty in such studies performed in an industrial context is that very few information is available on

the site and logs sampled since the trees and logs were already cut when we arrived for sampling.

We give below some examples of past uses of the database:

An automatic reading algorithm of the black and white calibration scale was designed by Delconte (2019).

Decelle and Jalilian (2020) proposed a neural network algorithm for automatic segmentation of the wood cross-section in the raw images taken in the forest or after transportation to Freiburg.

The superiority of convolutional neural networks for the identification of log cross-sections over methods adapted from fingerprint or iris recognition techniques was demonstrated in the comparative study by Wimmer et al. (2021a).

Convolutional neural networks were also used by Wimmer et al. (2021b) to identify a log from images taken by an RGB camera and a CT scanner.

Wimmer et al. (2022) shows that the use of hyperspectral imaging and the combination of several spectra provides significantly better results than RGB images alone regarding the visibility of growth rings, which are the main characteristic used for traceability.

Ravoajanahary et al. (2022) proposed a method for estimating tree ring density by coupling X-ray CT scanning and high-resolution optical measurements of tree ring width. This method was applied to analyse the relationship between ring density and ring width and cambial age at several height levels in the trees.

Acknowledgements

Thanks to *Forêt et Bois de l'Est* for helping us by providing the 100 spruce logs and by organizing log transportation to Freiburg. Thanks also to Martin Huber from *Forest Research Institute of Baden-Württemberg* (FVA) and all the team for helping us with the organization of log measurement and imaging at FVA.

Authors' contributions

FL initiated the funding request; managed the project for the French part; participated in the data collection, the data analysis and writing the manuscript; and supervised PhD and Master students. RS initiated the funding request, did his PhD thesis on the basis of these data and participated in the data collection, the data analysis and writing the manuscript. FM initiated the funding request and participated in the data collection, the data analysis and writing the manuscript. TR participated in the data collection, the data analysis and writing the manuscript. RD did his PhD thesis on the basis of these data and participated in the data collection, the data analysis and writing the manuscript. TC participated in the data collection, the data analysis and writing the manuscript. PN supervised the PhD and Master students and participated in the data analysis. IDR supervised the PhD and Master students and participated in the data analysis. KE supervised the PhD and Master students and participated in the data analysis. AP supervised the PhD and Master students and participated in the data analysis. FB participated in the data collection and writing the manuscript. AU initiated the funding request, managed the project for the Austrian part, participated in the data collection and supervised the PhD and Master students. All authors read and approved the final manuscript.

Funding

SilvaTech facility is supported by the French National Research Agency through the Laboratory of Excellence ARBRE (ANR-11-LABX-0002-01). This research was made possible thanks to the financial support of the French

National Research Agency (ANR) and the Austrian Science Fund (FWF) in the framework of the TreeTrace project, ANR-17-CE10-0016.

Availability of data and materials

The images and the database are available at Research Data Gouv repository: <https://doi.org/10.57745/WKLTJI>.

Code availability

Not applicable.

Declarations

Ethics approval and consent to participate

Not applicable.

Consent for publication

Not applicable.

Competing interests

The authors declare that they have no competing interests.

Received: 20 October 2022 Accepted: 25 January 2023

Published online: 13 February 2023

References

- BFW (2008) Bundesforschungszentrum für wald. (2008) bfw-praxisinformation nr. 16 - 2008. https://bfw.ac.at/030/pdf/1818_pi16.pdf. Accessed 11 Jan 2023.
- BFW (2022) Bundesforschungszentrum für wald. (2022) Österreichische waldinventur. periode 2016/21. <https://www.waldinventur.at>. Accessed 11 Jan 2023.
- Decelle R, Jalilian E (2020) Neural networks for cross-section segmentation in raw images of log ends. In: 2020 IEEE 4th International Conference on Image Processing, Applications and Systems (IPAS). IEEE, pp 131–137. <https://doi.org/10.1109/IPAS50080.2020.9334960>
- Delconte F (2019) Estimation de la qualité de grumes de bois. Master's thesis, M2 informatique, Parcours type Apprentissage, Vision, Robotique (AVR), Université de Lorraine, Nancy, France. <https://hal.univ-lorraine.fr/hal-03603108>
- FCBA (2022) Memento 2022. p 48. <https://www.fcba.fr/wp-content/uploads/2023/01/Memento-2022-WEB.pdf>. Accessed 11 Jan 2023.
- Freyburger C, Longuetaud F, Mothe F, Constant T, Leban JM (2009) Measuring wood density by means of x-ray computer tomography. *Ann For Sci* 66(8):804. <https://doi.org/10.1051/forest/2009071>
- Kurdthongmee W (2020) A comparative study of the effectiveness of using popular dnn object detection algorithms for pith detection in cross-sectional images of parawood. *Heliyon* 6(2). <https://doi.org/10.1016/j.heliyon.2020.e03480>
- Kurdthongmee W, Suwannarat K, Panyuen P, Sae-Ma N (2018) A fast algorithm to approximate the pith location of rubberwood timber from a normal camera image. In: 15th International Joint Conference on Computer Science and Software Engineering (JCSSE). IEEE, pp 1–6. <https://doi.org/10.1109/JCSSE.2018.8457375>
- Longuetaud F, Mothe F, Fournier M, Dlouha J, Santenoise P, Deleuze C (2016) Within-stem maps of wood density and water content for characterization of species: a case study on three hardwood and two softwood species. *Ann For Sci* 73(3):601–614. <https://doi.org/10.1007/s13595-016-0555-4>
- Longuetaud F, Pot G, Mothe F, Barthelemy A, Decelle R, Delconte F, Ge X, Guillaume G, Mancini T, Ravoajanahary T, Butaud JC, Collet R, Debled-Rennesson I, Marcon B, Ngo P, Roux B, Viguier J (2022a) Traceability and quality assessment of Douglas fir (*Pseudotsuga menziesii* (Mirb.) Franco) logs: the TreeTrace_Douglas database. *Ann For Sci* 79:46. <https://doi.org/10.1186/s13595-022-01163-7>
- Longuetaud F, Schraml R, Mothe F, Ravoajanahary T, Decelle R, Constant T, Ngo P, Debled-Rennesson I, Entacher K, Petutschnigg A, Brüchert F, Uhl A (2022b) "TreeTrace_spruce". [dataset]. Recherche Data Gouv. Repository, V1. <https://doi.org/10.57745/WKLTJI>
- Norell K (2011) Automatic counting of annual rings on *Pinus sylvestris* end faces in sawmill industry. *Comput Electron Agric* 75(2):231–237. <https://doi.org/10.1016/j.compag.2010.11.005>
- Norell K, Borgefors G (2008) Estimation of pith position in untreated log ends in sawmill environments. *Comput Electron Agric* 63(2):155–167. <https://doi.org/10.1016/j.compag.2008.02.006>
- Ravoajanahary T, Mothe F, Longuetaud F (2022) A method for estimating tree ring density by coupling CT scanning and ring width measurements: Application to the analysis of the ring width - ring density relationship in *Picea abies* trees. *Trees - Structure and Function*. <https://doi.org/10.1007/s00468-022-02373-2>
- Schraml R, Hofbauer H, Petutschnigg A, Uhl A (2015) Tree log identification based on digital cross-section images of log ends using fingerprint and iris recognition methods. In: *Computer Analysis of Images and Patterns. CAIP 2015. Lecture Notes in Computer Science*, vol 9256. Springer, pp 752–765. https://doi.org/10.1007/978-3-319-23192-1_63
- Schraml R, Uhl A (2013) Pith estimation on rough log end images using local fourier spectrum analysis. In: *Proceedings of the 14th Conference on Computer Graphics and Imaging (CGIM'13)*, Innsbruck, AUT. <https://doi.org/10.2316/P.2013.797-012>
- Schraml R, Uhl A (2014) Similarity based cross-section segmentation in rough log end images. In: *Artificial Intelligence Applications and Innovations. AIAI 2014. IFIP Advances in Information and Communication Technology*, vol 436. Springer, pp 614–623. https://doi.org/10.1007/978-3-662-44654-6_61
- Stängle SM, Brüchert F, Heikkilä A, Usenius T, Usenius A, Sauter UH (2015) Potentially increased sawmill yield from hardwoods using x-ray computed tomography for knot detection. *Ann For Sci* 72(1):57–65. <https://doi.org/10.1007/s13595-014-0385-1>
- Wimmer G, Schraml R, Hofbauer H, Petutschnigg A, Uhl A (2021a) Two-stage cnn-based wood log recognition. In: *Computational Science and Its Applications. ICCSA 2021. Lecture Notes in Computer Science*, vol 12955. Springer, pp 115–125. https://doi.org/10.1007/978-3-030-87007-2_9
- Wimmer G, Schraml R, Hofbauer H, Petutschnigg A, Uhl A (2022) An analysis of the use of hyperspectral data for roundwood tracking. In: *The 22nd International Conference on Computational Science and Its Applications (ICCSA 2022)*. Malaga, https://doi.org/10.1007/978-3-031-10545-6_21
- Wimmer G, Schraml R, Lamminger L, Petutschnigg A, Uhl A (2021b) Cross-modality wood log tracing. In: *2021 IEEE International Symposium on Multimedia (ISM)*. IEEE, pp 191–195. <https://doi.org/10.1109/ISM52913.2021.00038>

Publisher's Note

Springer Nature remains neutral with regard to jurisdictional claims in published maps and institutional affiliations.

Ready to submit your research? Choose BMC and benefit from:

- fast, convenient online submission
- thorough peer review by experienced researchers in your field
- rapid publication on acceptance
- support for research data, including large and complex data types
- gold Open Access which fosters wider collaboration and increased citations
- maximum visibility for your research: over 100M website views per year

At BMC, research is always in progress.

Learn more biomedcentral.com/submissions

